TRANSVERSE COHERENCE PROPERTIES OF A TGU-BASED FEL

Panagiotis Baxevanis, Zhirong Huang, Ronald Ruth, SLAC National Accelerator Laboratory, Menlo Park, CA 94025, USA
Carl B. Schroeder, Lawrence Berkeley National Laboratory, Berkeley, CA 94720, USA

Abstract

The use of a transverse gradient undulator (TGU) is considered an attractive option for FELs driven by electron beams with a relatively large energy spread. In this scheme, a dispersion is introduced in the beam while the undulator poles are inclined so that the undulator field acquires a linear dependence upon the transverse position in the direction of dispersion. By suitably selecting the dispersion and the field gradient, the energy spread effect can be significantly mitigated, thus avoiding a drastic reduction in the FEL gain. However, adding the dispersion typically leads to electron beams with large aspect ratios. As a result, the presence of higher-order modes in the output FEL radiation can become significant. To investigate this effect, we study the properties of the higher-order eigenmodes of a TGU-based, high-gain FEL, using both a simplified, analytically-solvable model and a variational technique. This formalism is then used to provide an estimate of the degree of transverse coherence for a representative soft X-ray, TGU FEL example.

INTRODUCTION

One of the most crucial parameters which affect the performance of a free electron laser (FEL) is the energy spread in the driving electron beam. A large value of the latter gives rise to a wide spread in the resonant wavelength, resulting in a substantially decreased FEL gain. Using a transverse gradient undulator (TGU) [1]- [2], it is possible to mitigate this problem. By dispersing the electron beam and tilting the undulator poles, both the electron energy and the undulator parameter acquire a linear transverse dependence. A suitable selection of the dispersion and the field gradient minimizes the impact of the energy spread upon the FEL resonance condition, leading to improved performance. This scheme has been shown to be attractive for FEL concepts that utilize the beam from laser-plasma accelerators (LPAs) [3]. However, a drawback of the TGU approach is the increased size of the electron beam in the direction of dispersion (typically the horizontal direction), which can cause the growth of multiple FEL modes in the exponential-gain regime, degrading the transverse coherence of the output radiation. In order to provide a theoretical framework for understanding this effect, we study the properties of the higher-order FEL modes for a TGU-based configuration. Our analysis is based on solving the FEL eigenmode equation for the parallel beam case (negligible emittance and focusing effects) by employing an exactly-solvable, approximate model and a variational approach. When applied to a specific LPA-based example, this formalism yields results which agree with simulation and provide us with insight into the factors which affect transverse coherence in a TGU FEL.

THEORY

As mentioned earlier, our study is based on an analysis of the FEL eigenmodes, i.e. the solutions of the form $A(\mathbf{x})e^{i\mu z}$ for the complex amplitude of the electric field of the radiation - where $\mathbf{x} = (x, y)$ is the transverse position vector and z is the longitudinal coordinate along the undulator. Each eigenmode is thus characterized by a z-invariant transverse profile $A(\mathbf{x})$ and a constant, complex growth rate μ. According to our previous treatment of a TGU-based FEL [4], the equation that is satisfied by the profile and the growth rate of a growing mode (i.e. one with $\mathrm{Im}(\mu) < 0$) in the parallel beam regime is

$$\left(\mu - \frac{\nabla_\perp^2}{2k_r}\right) A(\mathbf{x}) = U(\mathbf{x}, \mu) A(\mathbf{x}) , \tag{1}$$

where

$$U(\mathbf{x}, \mu) = -8\rho_T^3 k_u^3 \exp\left(-\frac{x^2}{2\sigma_T^2} - \frac{y^2}{2\sigma_y^2}\right) \times \int_{-\infty}^{0} d\xi \xi \mathrm{e}^{i(\mu - \Delta\nu k_u)\xi} e^{-2(\sigma_\delta^{ef})^2 k_u^2 \xi^2} \times \exp\left(-2ik_u C_p \frac{x}{\eta}\xi\right) . \tag{2}$$

Here, $\nabla_\perp^2 = \partial^2/\partial\mathbf{x}^2$, $k_r = 2\pi/\lambda_r$ and $k_u = 2\pi/\lambda_u$ - where λ_r is the resonant wavelength and λ_u is the undulator period - $\Delta\nu$ is a dimensionless detuning variable while σ_T and σ_y are the rms electron beam sizes in the x and y directions. The former of the last two parameters includes the contribution of the - constant - dispersion η and is given by $\sigma_T = (\sigma_x^2 + \eta^2\sigma_\delta^2)^{1/2}$, where σ_x is the non-dispersive horizontal beam size and σ_δ is the rms energy spread. Moreover, ρ_T and σ_δ^{ef} are, respectively, the effective Pierce parameter and energy spread of the FEL, quantities that are expressed by $\rho_T = \rho(1 + \eta^2\sigma_\delta^2/\sigma_x^2)^{-1/6}$ and $\sigma_\delta^{ef} = \sigma_\delta(1 + \eta^2\sigma_\delta^2/\sigma_x^2)^{-1/2}$, where ρ is the Pierce parameter for $\eta = 0$. This non-dispersive FEL parameter is in turn given by $\rho = (K_0^2[JJ]^2 I_p/(16 I_A \gamma_0^3 \sigma_x \sigma_y k_u^2))^{1/3}$, where γ_0 is the average electron energy in units of its rest mass m_0c^2, K_0 is the on-axis undulator parameter, $[JJ] = J_0(K_0^2/(4 + 2K_0^2)) - J_1(K_0^2/(4 + 2K_0^2))$, $I_A \approx 17$ kA is the Alfven current and I_p is the peak current of the electron beam. On the other hand, $C_p = \sigma_x^2/\sigma_T^2 + \bar{\alpha}\eta - 1$ with $\bar{\alpha} = K_0^2\alpha/(2 + K_0^2)$, α being the transverse gradient of the

ISBN 978-3-95450-133-5

undulator field. The expression for C_p given above is a generalization of the one contained in [4], which only covered the case with $\bar{\alpha} = 1/\eta$. The latter describes the TGU resonance condition. To proceed, we introduce the scaled quantities $\hat{x} = x/\sigma_T$, $\hat{y} = y/\sigma_y$, $\hat{\mu} = \mu/(2\rho_T k_u)$, $\hat{\xi} = 2\rho_T k_u \xi$, $\hat{\nu} = \Delta\nu/(2\rho_T)$ and $\hat{\sigma}_\delta^{ef} = \sigma_\delta^{ef}/\rho_T$, in which case the eigenmode equation is cast into a fully dimensionless form:

$$\left(\hat{\mu} - p_{dx}\frac{\partial^2}{\partial \hat{x}^2} - p_{dy}\frac{\partial^2}{\partial \hat{y}^2}\right) A(\hat{\mathbf{x}}) = \hat{U}(\hat{\mathbf{x}},\hat{\mu})A(\hat{\mathbf{x}}), \tag{3}$$

where $\hat{\mathbf{x}} = (\hat{x},\hat{y})$, $p_{dx} = (4\rho_T k_u k_r \sigma_T^2)^{-1}$ and $p_{dy} = (4\rho_T k_u k_r \sigma_y^2)^{-1}$ are the diffraction parameters,

$$\hat{U}(\hat{\mathbf{x}},\hat{\mu}) = -\exp\left(-\frac{\hat{x}^2}{2} - \frac{\hat{y}^2}{2}\right) \times \int_{-\infty}^{0} d\hat{\xi}\hat{\xi}e^{i(\hat{\mu}-\hat{\nu})\hat{\xi}}e^{-(\hat{\sigma}_\delta^{ef})^2\hat{\xi}^2/2}e^{-2i\hat{p}_0\hat{\xi}\hat{x}} \tag{4}$$

and $\hat{p}_0 = \sigma_T(C_p/\eta)/(2\rho_T)$.

Exactly Solvable Model

For $p_{dx}, p_{dy} \ll 1$, the radiation size in both the x and y directions is smaller than the corresponding size of the electron beam. In this case, we can expand the Gaussian term in the RHS of Eq. (4) according to $\exp(-\hat{x}^2/2 - \hat{y}^2/2) \approx 1 - \hat{x}^2/2 - \hat{y}^2/2$. Moreover, when $|\hat{p}_0| \ll 1$, the $\hat{\xi}$-integral in the definition of $\hat{U}$ can be approximated by $\hat{I}_0 - 2i\hat{p}_0\hat{I}_1\hat{x} - 2\hat{p}_0^2\hat{I}_2\hat{x}^2$, where $\hat{I}_n = \int_{-\infty}^{0} d\hat{\xi}\hat{\xi}^{n+1}e^{\Psi}$ and $\Psi = i(\hat{\mu}-\hat{\nu})\hat{\xi} - (\hat{\sigma}_\delta^{ef})^2\hat{\xi}^2/2$. Thus, by expanding $\hat{U}$ up to second order in $\hat{x}$ and $\hat{y}$, the mode equation is written in a simplified form as

$$\left(\hat{\mu} - p_{dx}\frac{\partial^2}{\partial \hat{x}^2} - p_{dy}\frac{\partial^2}{\partial \hat{y}^2}\right) A(\hat{\mathbf{x}}) = (F_0 + F_1\hat{x} + F_2\hat{x}^2 + G_2\hat{y}^2)A(\hat{\mathbf{x}}), \tag{5}$$

where $F_0 = -\hat{I}_0$, $F_1 = 2i\hat{p}_0\hat{I}_1$, $F_2 = \hat{I}_0/2 + 2\hat{p}_0^2\hat{I}_2$ and $G_2 = \hat{I}_0/2$. It can be shown that the above equation admits exact analytical solutions [5], which are given by

$$A_{mn}(\hat{\mathbf{x}}) = H_m(\sqrt{2\hat{a}_x}(\hat{x} - \hat{b}/(2\hat{a}_x)))e^{-\hat{a}_x\hat{x}^2+\hat{b}\hat{x}} \times H_n(\sqrt{2\hat{a}_y}\hat{y})e^{-\hat{a}_y\hat{y}^2}, \tag{6}$$

where H_k are the Hermite polynomials and $m,n = 0,1,2,\ldots$. The growth rate $\hat{\mu}$ and the mode parameters $\hat{a}_x, \hat{a}_y, \hat{b}$ satisfy the relations

$$\hat{\mu} + p_{dx}[(4m+2)\hat{a}_x - \hat{b}^2] + (4n+2)p_{dy}\hat{a}_y = -\hat{I}_0 \tag{7}$$

$$\hat{a}_x^2 = -\frac{\hat{I}_0 + 4\hat{p}_0^2\hat{I}_2}{8p_{dx}}, \quad \hat{a}_x\hat{b} = \frac{i\hat{p}_0}{2p_{dx}}\hat{I}_1, \quad \hat{a}_y^2 = -\frac{\hat{I}_0}{8p_{dy}}. \tag{8}$$

In general, the modes described by Eqs. (6)-(8) are characterized by an asymmetric intensity profile (given by $|A(\hat{\mathbf{x}})|^2$), which is not invariant under the reflection $x \to -x$, though it is still invariant under $y \to -y$. The main advantage of this model is that it provides a simple way to estimate the mode properties even for high mode order.

Variational Calculation

Approximations for the growth rate and the profile of an FEL mode can also be obtained through a well-established variational technique [6]. In this case, we begin by constructing a so-called variational functional, expressed by

$$\int d^2\hat{\mathbf{x}}A(\hat{\mathbf{x}})\left(\hat{\mu} - p_{dx}\frac{\partial^2}{\partial \hat{x}^2} - p_{dy}\frac{\partial^2}{\partial \hat{y}^2}\right)A(\hat{\mathbf{x}}) = \int d^2\hat{\mathbf{x}}A^2(\hat{\mathbf{x}})\hat{U}(\hat{\mathbf{x}},\hat{\mu}). \tag{9}$$

Given a trial function for the mode profile $A(\hat{\mathbf{x}})$, this functional yields an accurate estimate for the growth rate $\hat{\mu}$. Here, we seek to derive variational solutions for the first few eigenmodes. In order to make a judicious choice of the trial function for a specific mode, we each time try a form which has the same functional dependence on $\hat{x}$ and $\hat{y}$ as the exact solution given by Eq. (6). For example, we select a trial function of the form $A(\hat{\mathbf{x}}) = e^{-\hat{a}_x\hat{x}^2+\hat{b}\hat{x}}e^{-\hat{a}_y\hat{y}^2}$ for the fundamental (00, i.e. $m=0$, $n=0$) mode while our choice for the 01 mode is $A(\hat{\mathbf{x}}) = \hat{y}e^{-\hat{a}_x\hat{x}^2+\hat{b}\hat{x}}e^{-\hat{a}_y\hat{y}^2}$. Substituting these into Eq. (9), we obtain the result

$$F(\hat{a}_x,\hat{a}_y,\hat{b},\hat{\mu}) = \hat{\mu} + p_{dx}\hat{a}_x + \chi p_{dy}\hat{a}_y + (\hat{a}_x + 1/4)^{-1/2} \times \hat{a}_x^{1/2}\hat{a}_y^{\chi/2}(\hat{a}_y + 1/4)^{-\chi/2}\int_{-\infty}^{0} d\hat{\xi}\hat{\xi}e^{i(\hat{\mu}-\hat{\nu})\hat{\xi}}e^{-(\hat{\sigma}_\delta^{ef})^2\hat{\xi}^2/2} \times \exp\left(\frac{(\hat{b} - i\hat{p}_0\hat{\xi})^2}{2\hat{a}_x + 1/2} - \frac{\hat{b}^2}{2\hat{a}_x}\right) = 0, \tag{10}$$

where $\chi = 2n+1$, n being the second index of the 00/01 mode. Using the stationary condition $\partial\hat{\mu}/\partial\hat{a}_x = \partial\hat{\mu}/\partial\hat{a}_y = \partial\hat{\mu}/\partial\hat{b} = 0$, we also obtain the additional relations $\partial F(\hat{a}_x,\hat{a}_y,\hat{b},\hat{\mu})/\partial\hat{a}_x = 0$, $\partial F(\hat{a}_x,\hat{a}_y,\hat{b},\hat{\mu})/\partial\hat{a}_y = 0$ and $\partial F(\hat{a}_x,\hat{a}_y,\hat{b},\hat{\mu})/\partial\hat{b} = 0$. These three derivative relations have to be solved simultaneously along with Eq. (10) in order to determine the properties of the 00/01 mode. As far as the 10 mode is concerned, we now use a trial function of the form $A(\hat{\mathbf{x}}) = (\hat{x}+\hat{\lambda})e^{-\hat{a}_x\hat{x}^2+\hat{b}\hat{x}}e^{-\hat{a}_y\hat{y}^2}$ while, for the 11 mode, we choose $A(\hat{\mathbf{x}}) = (\hat{x}+\hat{\lambda})\hat{y}e^{-\hat{a}_x\hat{x}^2+\hat{b}\hat{x}}e^{-\hat{a}_y\hat{y}^2}$. These manipulations yield the relation

$$F(\hat{a}_x,\hat{a}_y,\hat{b},\hat{\lambda},\hat{\mu}) = (\hat{\mu} + \chi p_{dy}\hat{a}_y)\left[(\hat{\lambda} + \frac{\hat{b}}{2\hat{a}_x})^2 + \frac{1}{4\hat{a}_x}\right] + p_{dx}\hat{a}_x\left[(\hat{\lambda} + \frac{\hat{b}}{2\hat{a}_x})^2 + \frac{3}{4\hat{a}_x}\right] + \hat{a}_x^{1/2}(\hat{a}_x + 1/4)^{-1/2} \times \hat{a}_y^{\chi/2}(\hat{a}_y + 1/4)^{-\chi/2}\int_{-\infty}^{0} d\hat{\xi}\hat{\xi}e^{i(\hat{\mu}-\hat{\nu})\hat{\xi}}e^{-(\hat{\sigma}_\delta^{ef})^2\hat{\xi}^2/2} \times \left[(\hat{\lambda} + \frac{\hat{b} - i\hat{p}_0\hat{\xi}}{2\hat{a}_x + 1/2})^2 + \frac{1}{4\hat{a}_x + 1}\right] \times \exp\left(\frac{(\hat{b} - i\hat{p}_0\hat{\xi})^2}{2\hat{a}_x + 1/2} - \frac{\hat{b}^2}{2\hat{a}_x}\right) = 0, \tag{11}$$

where χ is defined as before. In this last two cases, the variational solution is completed by the relations $\partial F/\partial\hat{a}_x = \partial F/\partial\hat{a}_y = \partial F/\partial\hat{b} = \partial F/\partial\hat{\lambda} = 0$.

ISBN 978-3-95450-133-5

Table 1: Undulator and Electron Beam Parameters

Parameter	LPA
Undulator parameter K_0	2
Undulator period λ_u	1 cm
Beam energy $\gamma_0 m_0 c^2$	1 GeV
Resonant wavelength λ_r	3.9 nm
Peak current I_p	10 kA
Energy spread σ_δ	10^{-2}
Normalized emittance $\gamma_0\epsilon_x$	0.1 μm
Normalized emittance $\gamma_0\epsilon_y$	0.1 μm
Horizontal size σ_x	11.3 μm
Vertical size σ_y	11.3 μm
FEL parameter ρ	6×10^{-3}

NUMERICAL RESULTS

The formalism presented in the previous section can provide an estimate of the mode content in the output radiation from a TGU-based FEL. An interesting example of such a concept refers to a machine which would utilize a 1 GeV/10 kA LPA beam with the aim of producing radiation within the so-called water window wavelength region [3]. The full set of parameters is listed in Table 1. This set was also used in [4] in order to demonstrate the optimization of the dispersion η using a variational calculation for the fundamental FEL mode. The main results are summarized in the graph of the frequency-optimized gain length vs the dispersion (Fig. 1). In terms of our present scaling, the power gain length L_g is given by $L_g = -\sqrt{3}L_T/(2\text{Im}(\hat{\mu}))$, where $L_T = \lambda_u/(4\pi\sqrt{3}\rho_T)$. This optimization scenario involves varying the dispersion while keeping the other parameters fixed (except - of course - the TGU gradient, which satisfies the condition $\bar{\alpha} = 1/\eta$) and maximizing the power growth rate with respect to the detuning for each dispersion value. The optimum gain length is about 20 cm, for a 7 mm dispersion.

From a practical point of view, it may be desirable to select a dispersion value appreciably larger than the optimum. By thus moving away from the steep part of the optimization curve, the sensitivity of the gain length with respect to unexpected variations of η is reduced at a modest cost in terms of FEL gain. However, operating at or to the right side of the optimum typically creates an electron beam with a large ratio of horizontal to vertical size. As has been shown in simulation studies [3], such a configuration can allow the growth of multiple FEL modes in the high gain regime, reducing the transverse coherence of the output radiation. To study this effect, we first select a dispersion $\eta = 1$ cm (quite close to the optimum) and employ the variational solution in order to ascertain what the ordering of the various FEL modes is with respect to the power growth rate. For this dispersion value, $p_{dx} = 0.008$, $p_{dy} = 0.63$, $\hat{p}_0 = 0.02$ and the e-beam aspect ratio σ_T/σ_y is about 9. The main results are presented in Fig. 2, which shows the negative imaginary part of the scaled growth rate as a function of the detuning for the 00, 10, 01 and 11 modes. For each mode, the power growth rate attains a maximum for some negative detuning value. The corresponding frequency-optimized gain lengths are, respectively, $L_g^{00} = 20.4$ cm, $L_g^{10} = 21.2$ cm, $L_g^{01} = 30.5$ cm and $L_g^{11} = 32.3$ cm. The other important observation is that modes with the same n-index (and, thus, similar vertical profile) form groups with closely spaced growth rates. As expected, most favored are the modes with $n = 0$, which are characterized by Gaussian-like profiles and maximum overlap with the electron beam.

To check whether this pattern holds when more higher-order modes are included, we use the truncated, parabolic-like model to obtain equivalent detuning curves for the modes already considered plus some additional ones

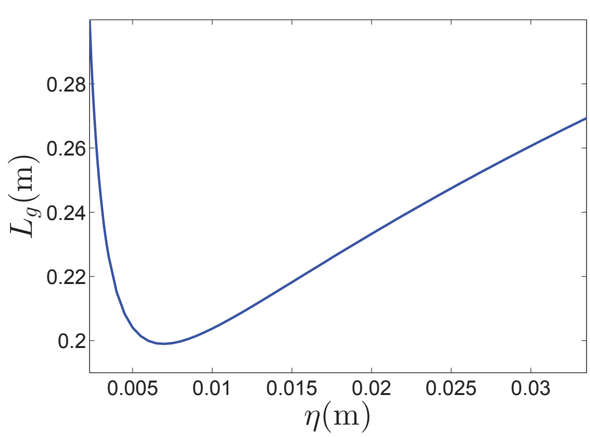

Figure 1: Frequency-optimized gain length of the fundamental mode as a function of the dispersion for the LPA parameters. The data shown were obtained using the variational solution.

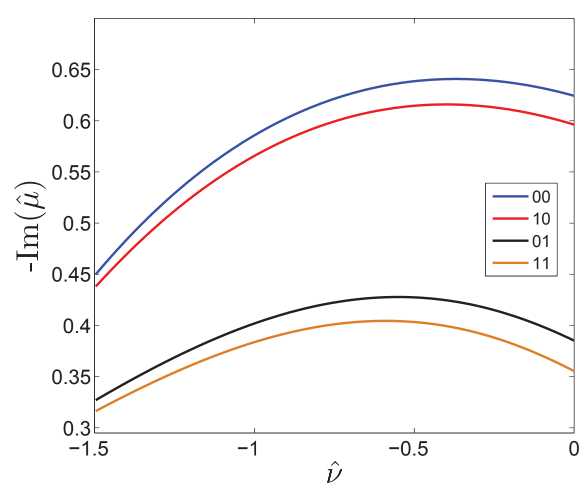

Figure 2: Negative imaginary part of the scaled growth rate $\hat{\mu}$ as a function of the scaled detuning $\hat{\nu}$ for various FEL modes (variational data for the $\eta = 1$ cm case).

ISBN 978-3-95450-133-5

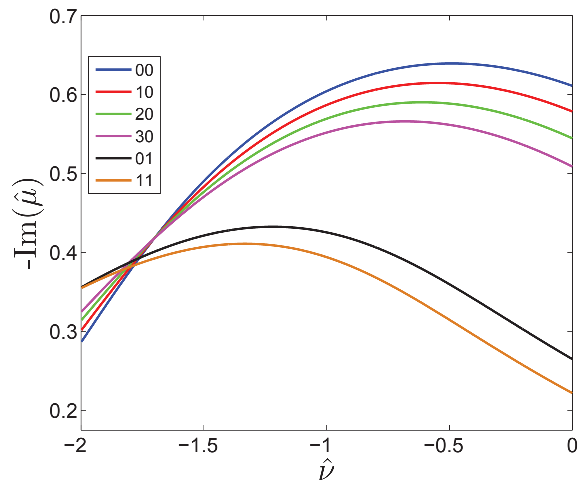

Figure 3: Negative imaginary part of the scaled growth rate $\hat{\mu}$ as a function of the scaled detuning $\hat{\nu}$ for several FEL modes (data from the analytical solution, for the η = 1 cm case).

(namely the 20 and 30 modes, see Fig. 3). We note that the data from the analytical solution are not identical to the variational results, as the detuning curves in the former case are shifted towards the left (i.e. the region of negative $\hat{\nu}$). This is due to the fact that, even though p_{dx} and $\hat{p}_0$ are much smaller than unity, p_{dy} is not quite so, with the result that the present parameters probably lie at the limit of the exact model's applicability. However, we can still verify that the mode spectrum has the same structure as in the variational case. Moreover, even though the detuning curves differ for the two approaches, both the variational and the exact solution actually give very similar estimates for the optimized gain lengths. For comparison, we now obtain L_g^{00} = 20.4 cm, L_g^{10} = 21.2 cm, L_g^{20} = 22.1 cm, L_g^{30} = 23.1 cm, L_g^{01} = 30.2 cm and L_g^{11} = 31.8 cm.

As a quantitative measure of the degree of transverse coherence, we use the quantities $f_{mn} = \exp(L_{sat}/L_g^{mn})/\exp(L_{sat}/L_g^{00})$. These express the ratio of the power amplification factor for the mn higher-order mode versus that of the fundamental at the saturation length L_{sat}. Since SASE - which is the operating mode assumed here - excites a range of frequencies, all gain lengths associated with this calculation are optimized with respect to the detuning. As an estimate of the saturation length, we use $L_{sat} = N_g L_g^{00}$, where $N_g \approx 20$. More precisely, we can use the formula $N_g \approx \log[P_{sat}/(P_{SASE}/9)]$, where $P_{sat} \approx 1.6\rho_T\gamma_0 m_0 c^2 I_p (L_T/L_g^{00})^2$ is the saturation power and $P_{SASE} \approx \rho_T^2 \gamma_0 m_0 c^3/\lambda_r$ is the SASE power [7]. For the 1 cm dispersion, this calculation yields $L_{sat} \approx 4.4$ m, which agrees with the simulated saturation within a 5 m undulator shown in [3]. Using the variational values for the mode gain lengths, we obtain $f_{10} \sim 0.43$, $f_{01} \sim 8\times10^{-4}$ and $f_{11} \sim 3.6\times10^{-4}$ while the values from the analytical solution yield $f_{10} \sim 0.43$, $f_{20} \sim 0.19$, $f_{30} \sim 8.5\times10^{-2}$, $f_{01} \sim 9.7\times10^{-4}$ and $f_{11} \sim 4.7\times10^{-4}$. These results would lead us to expect that at least 1-2 higher-order modes (10 and 20) would be visible in the radiation profile at saturation. Again, this is indeed what was observed in [3] for η = 1 cm. We have repeated this analysis for two additional dispersion values [5], namely η = 2 cm and η = 4 mm. The aspects ratios in these cases are ~ 18 and ~ 3.6, respectively, while σ_y is the same as before (~ 10 μm). In the first case, it was found that $f_{mn} \leq f_{10} \sim 0.68$ while the smaller dispersion yields $f_{mn} \leq f_{10} \sim 0.05$. This provides additional support for our main conclusion, which is that the transverse coherence for such TGU-based schemes is enhanced when the electron beam aspect ratio is decreased.

CONCLUSION

In this paper, we have developed a formalism that is suitable for investigating the higher-order mode properties of a TGU-based, high-gain FEL when emittance and focusing effects are negligible (parallel beam regime). We employ a variational approach along with an exactly solvable, parabolic-like model in order to obtain approximate solutions to the eigenmode equation, both for the fundamental and for the higher-order FEL modes. These solutions are then used in a study of the transverse coherence of the radiation from an LPA-based, TGU FEL example. Verifying earlier observations based on simulation, it is shown that a stronger TGU gradient (i.e. a smaller dispersion and thus less excessive horizontal beam size) enhances transverse coherence. This property is likely to be relevant in determining the operating parameters of a TGU FEL.

ACKNOWLEDGMENT

This work was supported by the Department of Energy Contract No. DE-AC02-76SF00515 and No. DE-AC02-05CH11231.

REFERENCES

[1] T. Smith, J. M. J. Madey, L. R. Elias and D. A. G. Deacon, J. Appl. Phys. 50, 4580 (1979).

[2] N. Kroll, P. Morton, M. Rosenbluth, J. Eckstein and J. Madey, IEEE J. Quantum Electron. 17, 1496 (1981).

[3] Z. Huang, Y. Ding and C. B. Schroeder, PRL 109, 204801 (2012).

[4] P. Baxevanis, Y. Ding, Z. Huang and R. Ruth, Phys. Rev. ST-AB 17, 020701 (2014).

[5] P. Baxevanis, Z. Huang, R. Ruth and C. B. Schroeder, to be submitted to Phys. Rev. ST-AB.

[6] M. Xie, Nucl. Instr. and Meth. A 507 (2003) 450.

[7] M. Xie, Nucl. Instr. and Meth. A 445 (2000) 67.